Computational Biology and Chemistry 117 (2025) 108437

Contents lists available at ScienceDirect

Computational Biology and Chemistry

journal homepage: www.elsevier.com/locate/cbac

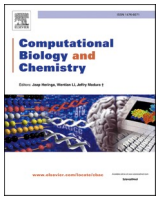

# Lung cancer detection and classification using optimized CNN features and Squeeze-Inception-ResNeXt model

Geethu Lakshmi G *, P. Nagaraj

*Department of Computer Science and Engineering, Kalasalingam Academy of Research and Education, Krishnankoil, Srivilliputhur, Tamil Nadu, India*

ARTICLE INFO

*Keywords:*
CT-scan
Deep learning
Lung cancer
Feature extraction
Optimization algorithm

ABSTRACT

Lung cancer, with its high mortality rate, is one of the deadliest diseases globally. The alarming increase in lung cancer deaths and its widespread prevalence have led to the development of various cancer control research and early detection methods aimed at reducing mortality rates. Effective diagnostic techniques are crucial for lowering lung cancer incidence, as early detection significantly impacts treatment success. Human error can often impede accurate identification of lung nodules, in which Computer-Aided Diagnostic (CAD) systems are utilized. These systems help radiologists by automating diagnostic processes and improving accuracy of detecting and classifying malignancies. This paper aims to develop a deep learning approach for classifying lung diseases using chest Computed Tomography (CT) scan images. The approach starts with image pre-processing, including color space conversion, data augmentation, resizing, and normalization. Feature extraction is carried out using a Convolutional Neural Network (CNN) optimized with Slime Mould Algorithm (SMA). For classification, a novel approach combining Squeeze-Inception V3 with ResNeXt, referred to as Squeeze-Inception-ResNeXt, is proposed. The Squeeze-Inception-ResNeXt model benefits from reduced computational cost while maintaining high performance in classifying lung diseases. This model categorizes lung diseases into Adenocarcinoma, Large Cell Carcinoma, and Squamous Cell Carcinoma. Additionally, SMA is utilized in training the Squeeze-Inception-ResNeXt model. Experimental results show that Squeeze-Inception-ResNeXt surpasses traditional models, with an accuracy of 97.7 %, sensitivity of 98.1 %, and specificity of 97.4 %.

## 1. Introduction

Lung cancer is a highly common and lethal cancer type globally, marked by an abandoned proliferation of lung cells. Prior findings are vital for lowering risk and enhancing survival rates, as lung cancer can develop over an extended period (Li et al., 2020a). Coupled with effective treatments, screening for pulmonary nodules can significantly improve patients' chances of recovery from lung cancer (Nair et al., 2024). The stage of cancer indicates the extent of its spread or metastasis. Stages 1 and 2 describe cancers that are confined to the lungs, while more advanced stages involve tumors that have spread to other organs (Schiller et al., 2019). Diagnostic approaches currently include biopsies and imaging techniques, like CT scans. Detecting lung cancer at an early stage greatly enhances the likelihood of endurance. However, prior-stage lung carcinomas are often more challenging to identify due to the limited presence of symptoms (Alakwaa et al., 2017). Radiologists use various techniques, including X-rays, CT scans, sputum cytology, and other MRI methods, to detect malignancies. Tumors fall into 2 categories: benign and malignant. Malignant tumors are cancerous, distinguished by their asymmetrical shapes and sizes, and tend to grow rapidly. Furthermore, research indicates that patients diagnosed at an advanced stage have significantly lower survival rates compared to

*Abbreviations:* DL, Deep Learning; ERWS, Enhanced Random Walker Segmentation; AI, Artificial Intelligence; GLCM, Gray-Level Co Occurrence Matrix; PCA, Principal Component Analysis; DSC, Dice Similarity Coefficient; SNN, Stacked Neural Network; MRI, Magnetic Resonance Imaging; FCL, Fully Connected Layer; TPR, True Positive Rate; CAD, Computer-Aided Diagnostic; RBF, Radial Base Function; CNN, Convolutional Neural Network; CT, Computed Tomography; GS-PCA, Graph-Based Sparse Principal Component Analysis; VGG, Visual Geometry Group; ANN, Artificial Neural Network; VOC, Volatile Organic Compounds; SMA, Slime Mould Algorithm; BN, Batch Normalization; SGL, Sparse Group Lasso; ReLU, Rectified Linear Unit; FCN, Fully Convolutional Network; H&E, Hematoxylin And Eosin; DCNN, Deep Convolutional Neural Network; E2E, End-To-End; FPR, False Positive Rate; NN, Neural Networks; SVM, Support Vector Machine; RF, Random Forest; ML, Machine Learning.

* Corresponding author.
*E-mail addresses:* geethu010@gmail.com (G. Lakshmi G), nagaraj.p@klu.ac.in (P. Nagaraj).

https://doi.org/10.1016/j.compbiolchem.2025.108437
Received 25 September 2024; Received in revised form 11 March 2025; Accepted 17 March 2025
Available online 25 March 2025

those diagnosed at an earlier stage (Mahum and Al-Salman, 2023).

A widely used imaging technique for detecting and diagnosing cancer is a CT scan. Radiologists, who are medical specialists responsible for interpreting these scans, classify lung lesions as either malignant or benign a chore that can be challenging and prone to errors. Lung lesions can vary greatly in shape, dimension, dissimilarity, and allocation, complicating the diagnostic process (Maleki and Niaki, 2023). The advent of CAD technologies has significantly enhanced accuracy and efficiency of medical diagnoses. These tools assist radiologists by increasing diagnostic precision through automated analysis. Automated lung cancer classification is particularly challenging due to the diverse imaging modalities used and the complex features of lung nodules (Dwivedi et al., 2014). CAD systems facilitate automatic identification of lung lesions in chest CT scans, addressing difficulties in diagnosing cancer by streamlining evaluation times and improving accuracy (Singh and Gupta, 2019). CAD process for lung cancer detection involves several phases, including preprocessing, segmentation, feature extraction, and categorization of lung lesions. Segmentation isolates nodules within CT scan, while classification determines whether a lesion is malignant or benign (Nair et al., 2024). Despite various existing approaches for segmenting and classifying lung nodules, AI-powered CT diagnostic systems have shown promise in accurately detecting lung cancer. This advancement holds noteworthy latent for improving lung carcinoma determination and may lead to broader clinical adoption (Crasta et al., 2024).

Several DL models have been presented for lung tumor determination, leveraging their ability to automatically extract features. Regardless of whether these models are based on segmentation or classification, their main advantage is automatic feature extraction facilitated by DL (Kalaivani et al., 2020). As depth of layers in these models increases, they can capture most representative features. DL models typically include pooling, BN, convolutional, and FCL. Pooling layers reduce the size of feature maps and simplify model. However, many current mechanisms confide in straightforward classification, which encompasses extracting features from an entire image (Mahum and Al-Salman, 2023). This approach can sometimes result in a higher rate of incorrect diagnoses, especially for early-stage tumors. Despite the potential for improved diagnostic accuracy and speed through DL techniques, several challenges remain. A significant hurdle is necessitating for immense aggregate of elevated-superiority information, which complicates accurate segmentation, annotation, and quality assurance. Automated techniques have been developed to handle these datasets, but they still require more precision (Alakwaa et al., 2017). Accurate lung cancer detection in medical imaging relies on detailed annotations, which demand substantial expert knowledge and time, impacting overall performance of DL models (Crasta et al., 2024).

The predominant objective of the study is to generate a DL method for classifying lung diseases using chest X-ray images. Images are preprocessed and SMA-based CNN is used for the feature extraction. Then, Squeeze-Inception V3 is used for lung cancer detection. Moreover, Squeeze-Inception V3 is combined with ResNext to propose Squeeze-Inception-ResNeXt for classification of lung diseases into Adenocarcinoma, Large cell carcinoma, and Squamous cell carcinoma. This integrates multiple transformations with consistent topology, resulting in improved accuracy and performance. Also, SMA is used in training the proposed Squeeze-Inception-ResNeXt, since SMA offers global optimization, robustness, efficiency, adaptability, and improving training accuracy and speed.

The primary contributions of the presented approach are:

- To design Squeeze-Inception-ResNeXt, is a combination of ResNeXt and Squeeze-Inception V3, for lung cancer diagnosis. ResNeXt has an advantage over other methods in this case since it combines many transformations with the same topology. Accuracy, great performance, and slow computing speed are all advantages of the Squeeze-Inception V3. To perform lung carcinoma diagnosis, the advantages of ResNeXt and Squeeze-Inception V3 are therefore combined in this work.
- Metrics, such as sensitivity, specificity, and accuracy are employed to evaluate the performance of the Squeeze-Inception-ResNeXt model.

**Organization of Paper:** Introduction is enclosed in 1st segment. 2nd segment provides a review of relevant literature. 3rd segment details proposed Squeeze-Inception-ResNeXt model for lung cancer detection. Findings and discussion are covered in 4th segment, and 5th segment concludes the study.

## 2. Literature survey

This section examines existing literature on various methods used for lung cancer detection. Selected studies are evaluated based on their advantages and limitations in context of identifying lung cancer.

Crasta et al. (2024) suggested DL architecture for perceiving and diagnosing lung carcinomas through the analysis of CT images. Their method involves a CNN designed to identify and classify lung nodules with high precision. The architecture integrates advanced image preprocessing techniques to enhance the quality of CT scans before feeding them into the CNN. By leveraging a multi-layered network structure and sophisticated feature extraction methods, the proposed model aims to improve diagnostic accuracy, reduce false positives, and provide timely detection of lung carcinomas. BR et al. (2024) identified prior phase of lung carcinomas and assessed accuracy levels of several NN. Initially, image processing methods are used to extract lung regions. For the segmentation process, SNN is employed. Once features are extracted from the segmented images, different neural network methods are utilized for the classification task.

Li et al. (2024) utilized a hybrid feature extraction strategy that combines autoencoder features with an autoencoder and GLCM with Haralick. Following that, supervised machine learning techniques were trained using these features. While SVM polynomial provided superior accuracy and reached flawless performance metrics. These outcomes show how the suggested strategy may be used to create better prognostication and symptomatic tools for lung carcinoma medicament planning and decision-making. Nair et al. (2024) recommended an enhanced lung cancer detection technique that unites ERWS with ANN and RF classifiers. The process begins with enhanced random walker segmentation to accurately delineate lung structures and identify potential cancerous regions. Features extracted from the segmented images are then fed into a hybrid classification system. This approach aims to leverage the strengths of both classifiers, improving detection accuracy and robustness. The proposed method is designed to provide more precise and reliable lung cancer diagnosis from medical imaging.

Mahum and Al-Salman (2023) presented a method for lung carcinomas determination utilizing a RetinaNet architecture. The approach involves using RetinaNet, a well-known object detection network and integrates it with a multi-scale feature fusion technique to capture detailed information at various scales. Additionally, a context module is employed to incorporate contextual information from the images, improving detection accuracy. The method is designed to effectively identify and localize cancerous lesions in lung CT scans, aiming to enhance overall diagnostic performance and reliability. Liu et al. (2021) suggested a lung carcinomas determination method using an electronic nose to analyze breath samples. Their approach is improved with sparse group feature selection, which optimizes the process by focusing on the most relevant biomarkers and reducing noise. This technique improves detection accuracy and efficiency, offering a non-invasive and practical solution for early lung cancer diagnosis through advanced breath analysis.

Ram et al. (2023) suggested a method for lung carcinoma lesion determination in histopathology images using a graph-based sparse PCA network. Their approach employs sparse PCA within a graph-based framework to enhance feature extraction and lesion detection. This

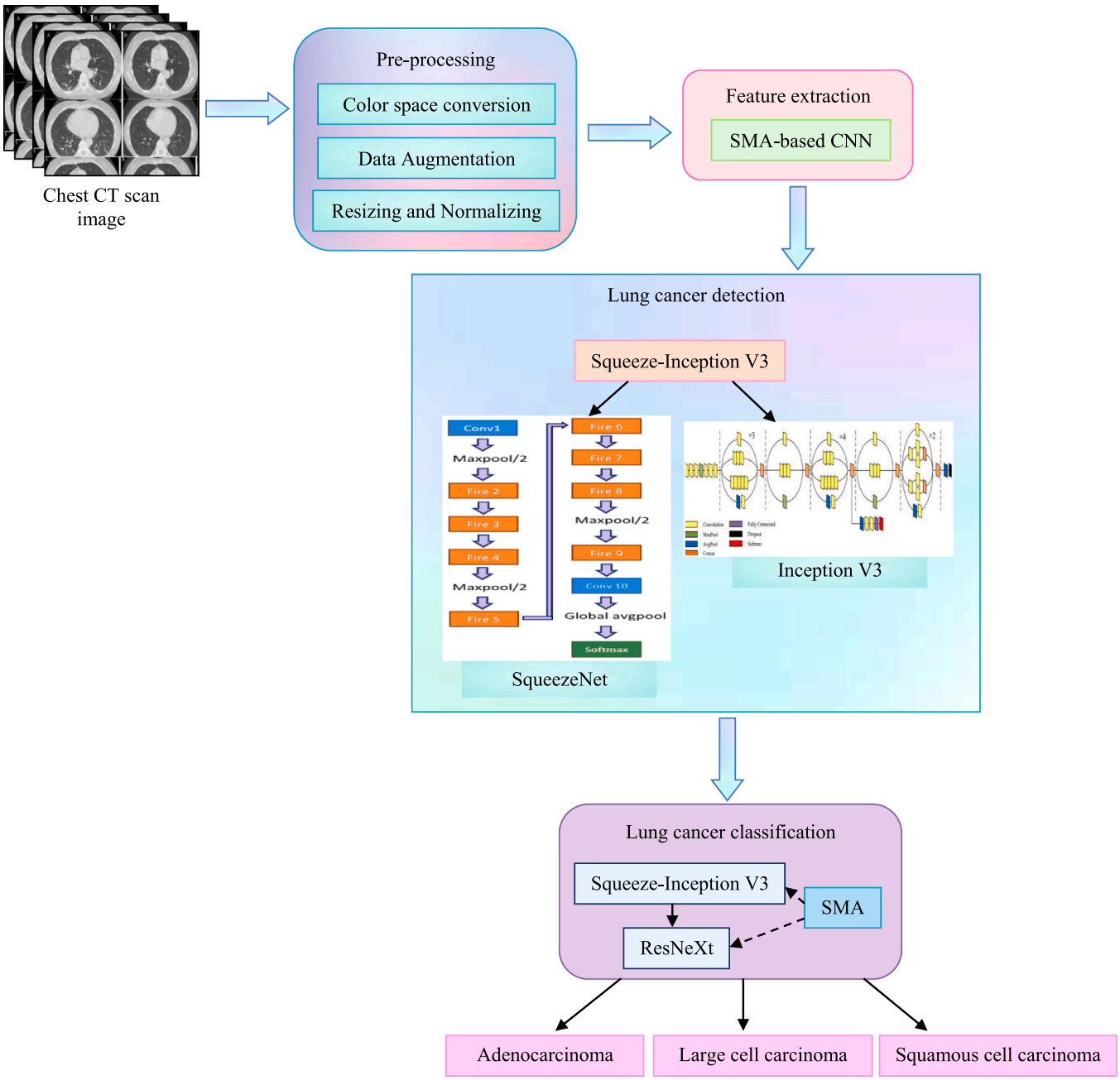


**Fig. 1.** Structural representation of proposed Squeeze-Inception-ResNeXt for lung cancer detection and classification.

technique aims to capture the complex structures and variations in histopathology images effectively. By integrating graph-based methods with sparse PCA, the network improves the detection accuracy of lung cancer lesions, facilitating more precise diagnosis and treatment planning in histopathological evaluations. Ozdemir et al. (2019) introduced CAD and distinguishing epitome that originates consequential likelihood assessments for lung carcinomas screening with low-dose CT scans. This approach, relying solely on 3D CNN, demonstrated enhanced performance in detecting lung nodules and classifying malignancies. Integration of analysis and detection models was essential, as it enabled development of an end-to-end methodology with enhanced and additional consistent outcomes, eliminating need for separate phases of false positive reduction and nodule determination.

### 2.1. Motivation

The increasing prevalence of lung diseases, chiefly lung cancer, needs the development of accurate, automated methods for early recognition from CT scan images. Manual diagnosis is time-consuming and prone to human error, and there is a pressing require for automated systems that can help healthcare professionals. Issues with conventional methods outlined in previous segment highlight preceding research gaps:

- CNN used in Crasta et al. (2024) demonstrated high performance but did not improve the model's clarity and comprehensibility. Additionally, while SNN employed in BR et al. (2024) did not enhance classification accuracy, there is potential to further strengthen the model's robustness.

- Although RetinaNet excels at detecting tumors by extracting important features from images, its ability to identify small tumors is reduced due to limited resolution of input images (Mahum and Al-Salman, 2023).
- Additionally, lack of visual analysis of learned feature representations by CNN (Ozdemir et al., 2019) obstructs the timely evaluation and explication of CAD results.

This work addresses these challenges by presenting an efficient deep learning approach to classify lung diseases, which presents the potential for faster, more accurate diagnoses.

## 3. Proposed Squeeze-Inception-ResNeXt for lung disease classification

This study proposes a DL method for recognizing lung diseases using chest CT scan images. The framework for the classification of lung disease is illustrated in Fig. 1. The process begins with image pre-processing, which includes color space conversion, data augmentation, resizing, and normalization. Subsequently, feature extraction is performed on pre-processed images using a CNN optimized with SMA. Next, Squeeze-Inception V3 is augmented for lung cancer detection, leveraging the benefits of both models, including enhanced accuracy, high performance, and reduced computational requirements. Additionally, Squeeze-Inception-ResNeXt, where Squeeze-Inception V3 combined with ResNext is proposed for classifying lung diseases into Adenocarcinoma, Large Cell Carcinoma, and Squamous Cell Carcinoma. This integrates multiple transformations with consistent topology, resulting in improved accuracy and performance, though it may exhibit slower computational speed. Furthermore, SMA is employed in training the proposed Squeeze-Inception-ResNeXt model, which is designed for lung cancer classification. SMA offers global optimization, robustness, efficiency, and adaptability, improving training accuracy and speed.

### 3.1. Pre-processing the chest X-ray Images

Pre-processing is applied to lung images to enhance clarity and contrast by reducing noise. The main aim is to smooth the images, achieved through techniques such as color space conversion, data augmentation, normalization, and scaling. Images from databases, which vary in size and color depth within the [0,255] pixel range, are first converted to RGB. They are then resized to 256 × 256 pixels and normalized to a range of 0–1.

#### 3.1.1. Color space conversion

This involves changing an image's color representation from one format to another. The goal is to produce an image that maintains the original's appearance as closely as possible (Bi and Cao, 2021). For example, in the YCbCr color model, the "Y" component represents luminance, while "Cr" and "Cb" represent the chrominance, indicating the intensities of red and blue relative to green.

#### 3.1.2. Data augmentation

Using an artificial dataset created by modifying a standard dataset, data augmentation methodology is used to raise quantity of images. Here, three augmentation techniques that are most frequently employed namely, vertical flip, horizontal flip, and 90° rotation are applied (Alnowami et al., 2022). Horizontal flip augmentation randomly flips the input image with a set probability along its vertical axis. Additionally, the input image is arbitrarily and with a certain probability flipped along its horizontal axis by the vertical flip augmentation. Rotation in data augmentation involves rotating images by specified angles to increase the variability of training data. This technique helps model generalize better by exposing it to different orientations of the same image, thereby improving its ability to distinguish objects apart from their arrangement or configuration in input data. Following the augmentation process, final set of preprocessed images comprises 7007 samples, ready for use in training DL models.

#### 3.1.3. Resizing and normalizing

Images are resized by nearest neighbor interpolation method to a specified output size from various detection approaches (Dharavath et al., 2014). This resizing, along with normalization, is performed during the pre-processing stage. It includes adjusting pixel intensity values to a range of 0–1 and standardizing the image dimensions.

### 3.2. SMA-based CNN features

This section offers an in-depth analysis of CNN features utilizing the SMA. It employs a CNN model optimized with SMA for feature extraction (Kumar and Kukreja, 2021). One significant advantage of CNNs is their competence to discover forthwith from raw pixel data, thus removing the necessitate for physical feature extraction. Furthermore, using optimization techniques can enhance performance of feature extraction. Thus, the work leverages the capabilities of SMA-CNN for enhanced feature extraction. A critical component used for lung carcinoma determination from pre-processed images is the CNN. CNN comprises 3 main layers: convolutional layer, pooling layer, and FCL. The first step in CNN framework involves extracting features from convolutional layer, which analyzes pre-processed images. This layer preserves the spatial relationships between pixel values and image features (Kumar and Kukreja, 2021).

#### 3.2.1. Convolution layer

The convolutional layer primarily applies a filter or mask to an image to produce a matrix as output. This can be expressed as follows:

$$Y_e = J \otimes H_e + d_e \tag{1}$$

wherein, $J$ is the pre-processed image, $H_e$is the $e$thconvolution kernel in CL, $d_e$signifies bias term, $\otimes$ convolution operation and $Y_e$ is $e$th output feature map.

The resultant feature map was subjected to a non-linear activation function after the convolution operation to introduce non-linearity. The aforementioned operation is as follows:

$$K_{i,j} = q\left(\sum_{t=0}^{M-1}\sum_{w=0}^{N-1}\sum_{l=0}^{N-1} P_{w,l,t} * P_{w,l,t} * X_{i+w,j+l+j,t} + d\right) \tag{2}$$

wherein, non-linear activation function is denoted by $q(.)$, output feature map node at location $(i,j)$is signified by $K_{i,j}$, size of convolution kernel is $N \times N$,$P_{w,l,t}$, input pixel value is represented by $X_{i+w,j+l+j,t}$and$d$denotes the network performance.

#### 3.2.2. Activation function

An activation function is a mathematical function used in neural networks to introduce non-linearity and enable the model to learn complex patterns. This transformation is achieved using the ReLU activation function, which processes the matrix to produce the final vector representation.

#### 3.2.3. Pooling layer

The purpose of this layer is to minimize the dimension of constraint. Common methods for feature reduction include min, max, and average pooling. Mathematically, it is described as follows:

$$O_{i,j,e} = P^{L}_{(W,l)} \in I_{i,j}(c_{w,l,e}) \tag{3}$$

where, $P^L$signifies pooling operation, $O_{i,j,e}$denotes new value at location of$(i,j)$in $e^{th}$feature map after pooling operation, $I_{i,j}$refers to pooling region around location $(i,j)$, and$c_{w,l,e}$ is node at location$(i.j)$within pooling region.

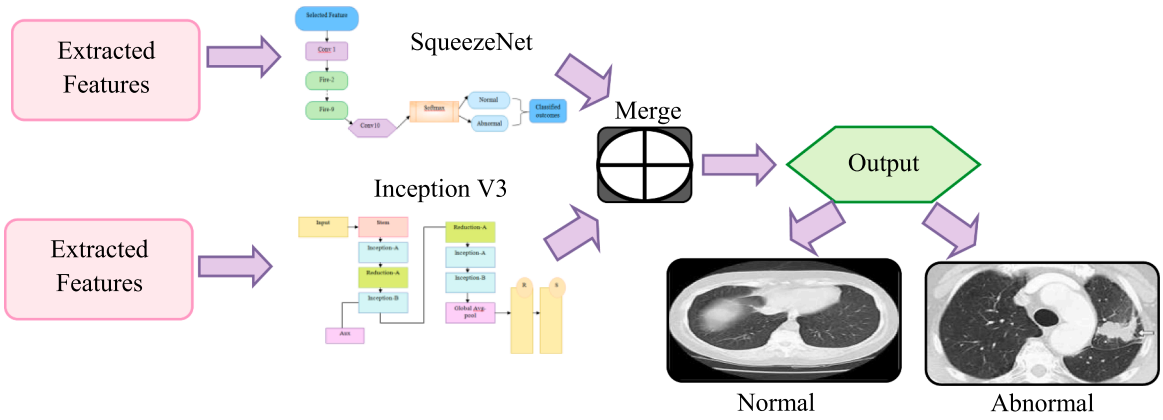


**Fig. 2.** Architecture of SqueezeNet-InceptionV3-based lung cancer detection.

#### 3.2.4. Dropout

Dropout is a regularization technique where random neurons are temporarily removed during training to prevent overfitting. The training data might not always be appropriate for testing protocols. Under- and over-fitting issues are resolved with the dropout technique.

#### 3.2.5. Fully connected layer

Since each neuron in an FCL of a neural network is related to every other neuron in layer above, a model can learn complex representations.

#### 3.2.6. Softmax

Softmax is a function that converts a vector of values into a probability distribution, where each value is represented as a proportion of the total. It may manifest as characteristics that are shaped, colored, or have textures. These characteristics are therefore used for classification and prediction. The softmax activation function's mathematical expression is as follows:

$$f = SMX(H_n \circ r + B_A) \tag{4}$$

wherein, $f$is predicted class, $H_n$is value of hidden neurons, $\circ$ indicates element wise multiplication, $r$denotes weight matrix connecting the FCL to output layer, and $B_A$represents bias term.

The CNN algorithm, which is stimulated by the slime mold performance's natural fluctuations, is adjusted using SMA. Adaptive weights are used in SMA to imitate biological waves by integrating a variety of fresh features and unique parameters (Li et al., 2020b). Through its capacity for exploration and exploitation, the SMA offers the best route to link food sources. Based on the order in the air, slime mold can migrate in the direction of food. SMA offers global optimization, robustness, efficiency, adaptability, and improving training accuracy and speed.

### 3.3. SqueezeNet-Inception V3-based lung cancer detection

This section describes the Hybrid SqueezeNet-Inception V3 cancer detection process in full. Primary advantage of SqueezeNet model resides in its capacity to uphold equilibrium between processing resources and accuracy. Inception V3 was primarily concerned with cutting down on calculation time through the improvement of the earlier Inception frameworks, leading to increased effectiveness and improved network convergence. To detect lung cancer, SqueezeNet and Inception V3 are hybridized.

#### 3.3.1. SqueezeNet

SqueezeNet is a CNN designed to achieve performance comparable to AlexNet while using 50 times fewer parameters. It features multiple fire modules, each consisting of a squeeze convolution layer proceeding by a developed layer that takes input from squeeze layer. SqueezeNet improves computational efficiency without sacrificing accuracy (Zhu et al., 2022). Network starts with a convolutional layer, processes through 8 fire modules, and concludes with a final convolutional layer, followed by 2 stages of max-pooling. To reduce number of parameters while preserving accuracy, SqueezeNet uses a convolutional kernel strategy and substitutes fully connected layers with an average pooling layer.

#### 3.3.2. Inception V3

Google developed InceptionV3 model as an advanced iteration of original Inception network, aimed at improving image classification accuracy. This approach enables InceptionV3 to expand both width and depth of the network without additional computational overhead (Meena et al., 2023). Redundancy and inefficiency are addressed by architecture through the use of a twenty-two-layer sparse CNN structure and parallel processing methodology. In order to improve discriminative ability of lower layers, it additionally incorporates auxiliary classifiers. InceptionV3 is able to apply both pooling and convolutional operations simultaneously at each layer, in contrast to conventional CNNs, like VGG and AlexNet, which only execute one of these operations at a time.

Initially, SqueezeNet and Inception V3 models are run separately on extracted features. Their outputs are then combined using a merge layer to capitalize on the strengths of both models. This merging process integrates their advantages through operations like addition, and improving representation of input data. Combined features are subsequently used for lung cancer diagnosis. Fig. 2 depicts architecture of SqueezeNet-Inception V3 model designed for diagnosing lung cancer.

### 3.4. SMA based Squeeze-Inception-ResNeXt Lung cancer classification

In this section, Squeeze-Inception-ResNeXt, proposed using Squeeze-Inception V3 combined with ResNext, for the lung cancer classification into Adenocarcinoma, Large cell carcinoma, and Squamous cell carcinoma, is described. Also, SMA is used in training the proposed Squeeze-Inception-ResNext. Integrating SMA in Squeeze-Inception-ResNeXt creates a powerful and efficient model capable of high performance, effective feature learning, and scalability, making it well-suited for various advanced computer vision tasks and real-time applications.

#### 3.4.1. ResNeXt

ResNeXt is a DL architecture that builds upon the ResNeXt framework by introducing a concept called cardinality. It employs grouped convolutions, where each group processes data independently before merging, allowing the network to capture more diverse features without significantly increasing computational cost (Xie et al., 2017). ResNeXt's design enhances the network's ability to learn complex patterns and improves performance on tasks such as image classification. By balancing depth and width with cardinality, ResNeXt achieves elevated

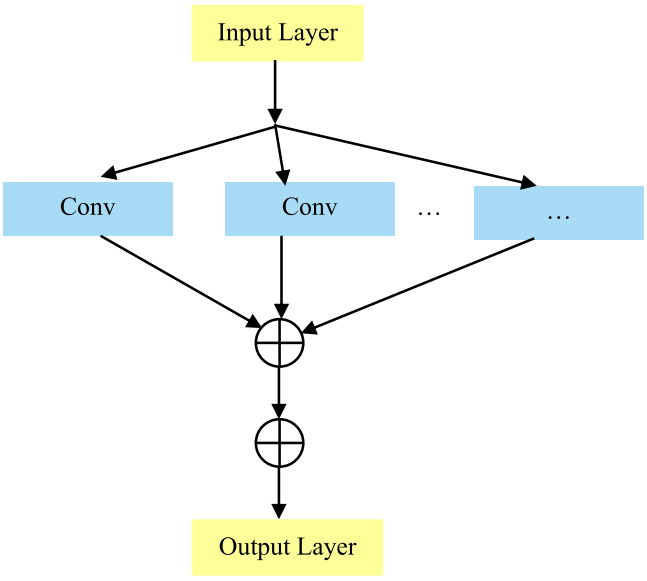


**Fig. 3.** Structure of ResNeXt model.

accuracy and efficiency, forecasting it a popular selection in modern computer vision applications. The combined transformation is displayed as,

$$C(h) = \sum_{m=1}^{u} Q_{n(g)} \tag{5}$$

Residual function is integrated transformation illustrated by,

$$o = g + \sum_{m=1}^{u} Q_{n(g)} \tag{6}$$

where, $Q_{n(g)}$is arbitrary function,$u$ denotes cardinality and$o$ is output. The output of SqueezeNet-Inception V3-ResNeXt is given by,

$$Z_2 = \left[ g + \sum_{m=1}^{u} Q_{n(g)} \right] \otimes A_{y.k} \otimes Z_1 \tag{7}$$

wherein, $A$denotes input data, and $Z_1$represents SMA-based SqueezeNet-Inception V3 output. Fig. 3 shows the ResNeXt model.

a) ***Map Layer***

This processes spatial data from input images or other spatially structured inputs. It typically involves operations like convolution, pooling, or other transformations to extract and refine features across different spatial locations. This layer is crucial for capturing patterns and structures in data, contributing to the model's ability to understand spatial hierarchies.

$$S_{t+1} = \sum_{x=1}^{v} (F_x * We_x) \tag{8}$$

wherein, $F$ reveals extracted features and $We$ reveals linear regression weight.

b) ***Merging Layer***

The merging layer combines outputs from multiple layers or models to integrate diverse features and improve overall performance. It typically employs operations like concatenation, addition, or averaging to blend different feature representations. This integration helps in creating a more comprehensive and robust representation of improving ability of model to formulate accurate forecasting and input data.

$$Z_3 = S_{t+1} + Z_2 * We \tag{9}$$

$$Z_3 = \sum_{x=1}^{v} (F_x * We_x) + \left[ g + \sum_{m=1}^{u} Q_{n(g)} \otimes A_{y.k} \otimes Z_1 \right] * We \tag{10}$$

Here, the SMA is used to update the parameter of the ResNeXt. Fig. 4 provides a depiction of the structure of the proposed method.

## 4. Results

This section details the experimental analysis of presented model. An analysis is conducted using PYTHON tool, with performance metrics including accuracy, sensitivity, and specificity applied to assess the model's effectiveness.

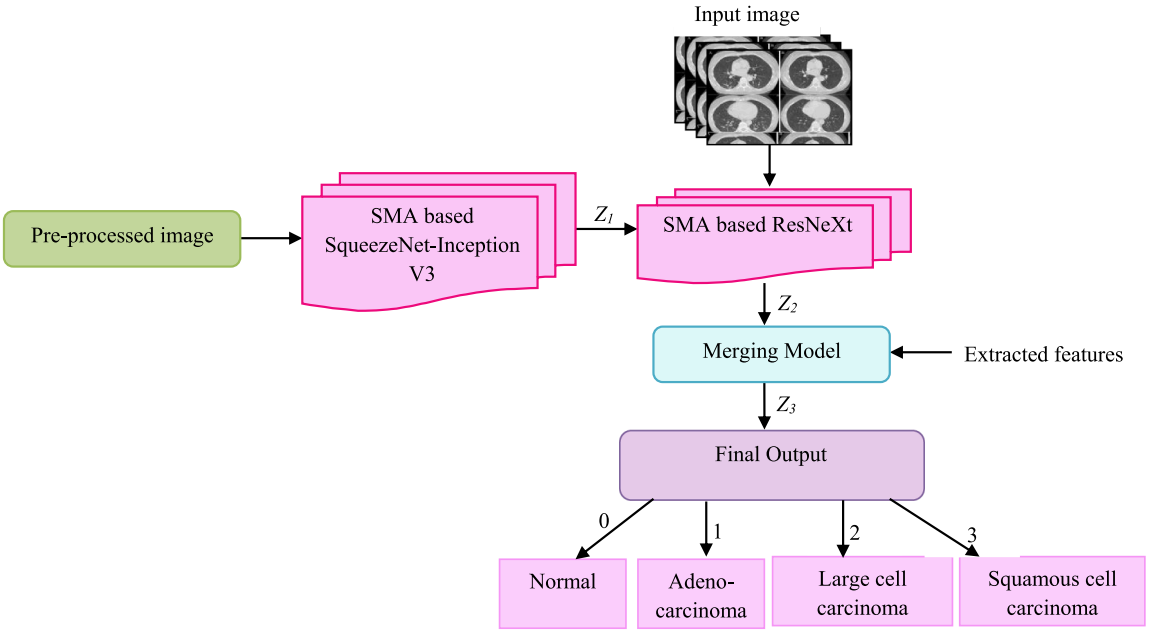


**Fig. 4.** A diagram of proposed method structure.

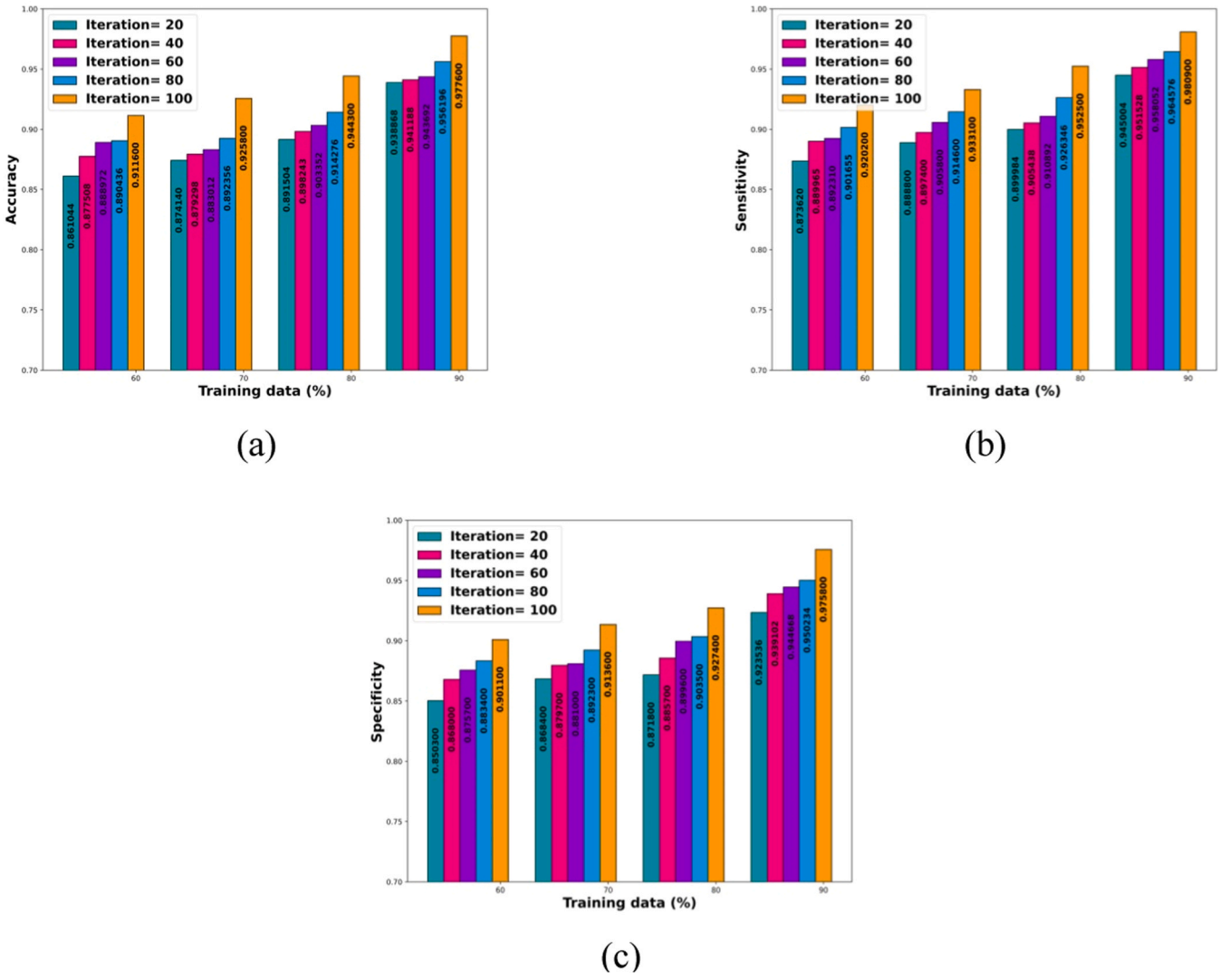


**Fig. 5.** Performance analysis for (a) accuracy, (b) sensitivity, and (c) specificity.

### 4.1. Dataset description

Chest CT scan images utilized in this study are acquired from a publicly available dataset on Kaggle (Chest CT-Scan images Dataset). This dataset comprises 967 carefully selected CT scans, each rigorously labeled through comprehensive verification. The images are classified into four specific categories for lung cancer detection: large-cell carcinoma, adenocarcinoma, normal cases and squamous cell carcinoma.

### 4.2. Performance metrics

This portion evaluates measurements used to analyze method performance using conventional strategies:

a) ***Accuracy***

Percentage of correctly identified cases relative to total number of examples is known as accuracy.

$$\alpha = \frac{T_{POS} + T_{NEG}}{T_{POS} + T_{NEG} + F_{POS} + F_{NEG}} \tag{11}$$

where, $\alpha$ represents accuracy, $T_{POS}$reveals true positive, $T_{NEG}$ reveals true negative, $F_{POS}$ reveals false positive, $F_{NEG}$ reveals false negative.

b) ***Specificity***

Out of all actual negatives, specificity quantifies the percentage of true negatives that are accurately identified.

$$\beta = \frac{T_{POS}}{T_{POS} + F_{POS}} \tag{12}$$

where, $\beta$represents sensitivity.

c) ***Sensitivity***

Sensitivity quantifies the percentage of accurately diagnosed true positives among actual positives.

$$\eta = \frac{T_{NEG}}{T_{NEG} + F_{NEG}} \tag{13}$$

where, $\eta$reveals specificity.

### 4.3. Performance analysis

A performance study of specificity, sensitivity, and accuracy for presented technique is exposed in Fig. 5. Evaluating performance according to accuracy is shown in Fig. 5(a). Squeeze-Inception-ResNeXt technique performed accurately (0.874) at 70 % of training data at iteration 20 and attained accuracy of 0.892 at iteration 80. Squeeze-Inception-ResNeXt achieved error rates of 0.944 at iteration 60 and

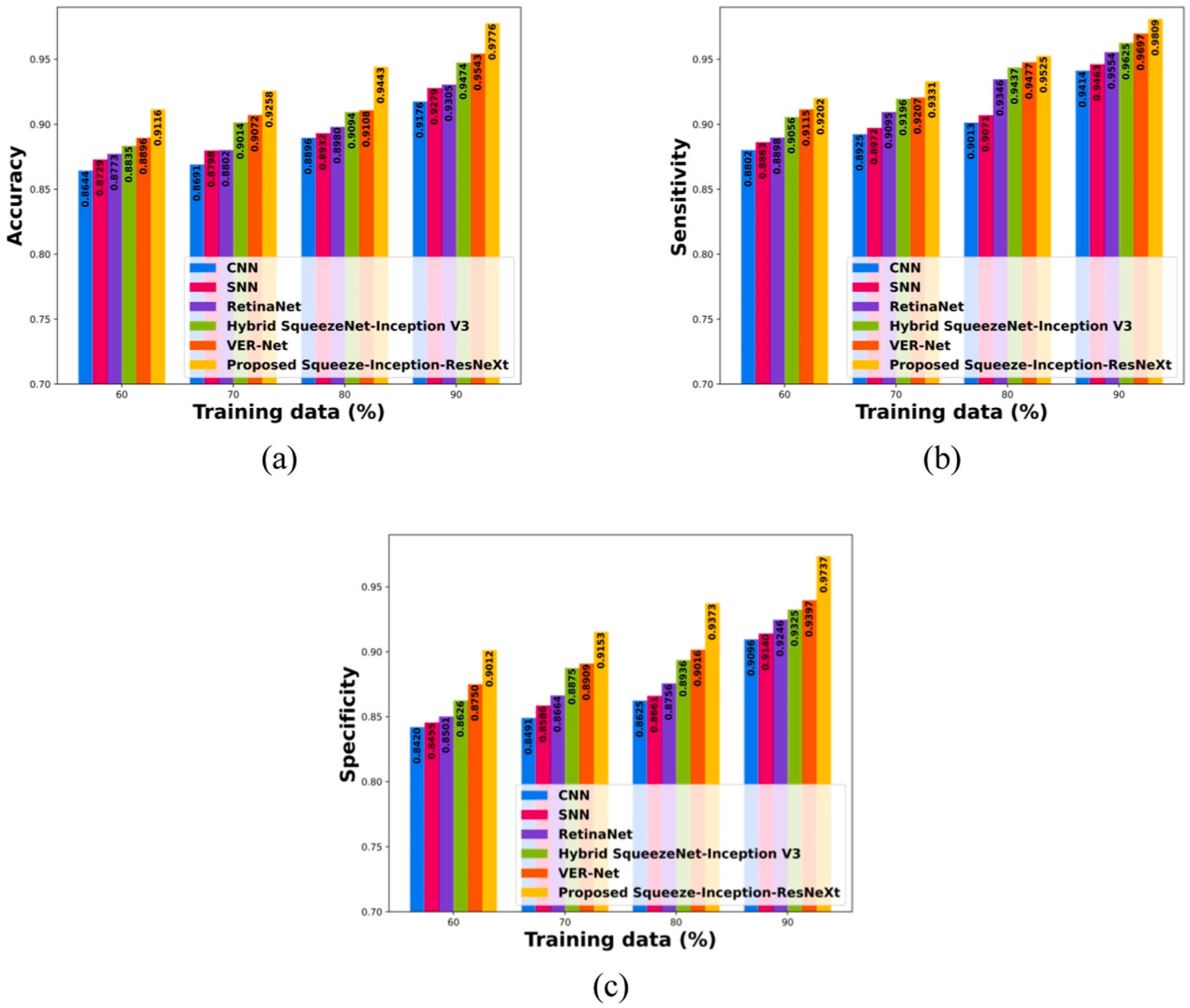


**Fig. 6.** Comparative analysis for (a) accuracy, (b) sensitivity, and (c) specificity.

0.978 at iteration 100 for training data 90 %. Performance assessment according to sensitivity is exhibited in Fig. 5(b). At iteration 20, Squeeze-Inception-ResNeXt technique achieved a sensitivity of 0.945, and at iteration 60, it reached 0.958 for training data 90 %. Squeeze-Inception-ResNeXt exhibited a sensitivity of 0.892 at iteration 60 and 0.902 at iteration 80 when dealing with 60 % training data. Performance is estimated according to specificity, exposed in Fig. 5(c). A specificity of 0.886 was reached by Squeeze-Inception-ResNeXt at iteration 40 and 0.937 at iteration 100 for training data 80 %.

### 4.4. Comparative analysis

Comparative assessment of the described mechanism in relation to conventional methods like CNN (Crasta et al., 2024), SNN (BR et al., 2024), RetinaNet (Mahum and Al-Salman, 2023), VER-Net (Saha et al., 2024), and Hybrid SqueezeNet-Inception V3 and Proposed Squeeze-Inception-ResNeXt is enclosed in this segment.

Fig. 6 displays a comparison analysis based on Squeeze-Inception-ResNeXt for specificity, sensitivity, and accuracy for various training datasets on different methods. Accuracy comparing evaluation was exposed in Fig. 6(a). With 90 % training data, proposed Squeeze-Inception-ResNeXt method achieved an accuracy of 0.977, whereas

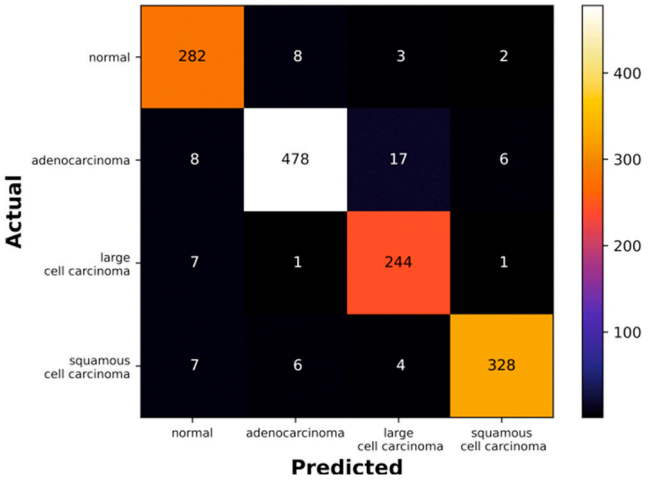


**Fig. 7.** Representation of confusion matrix.

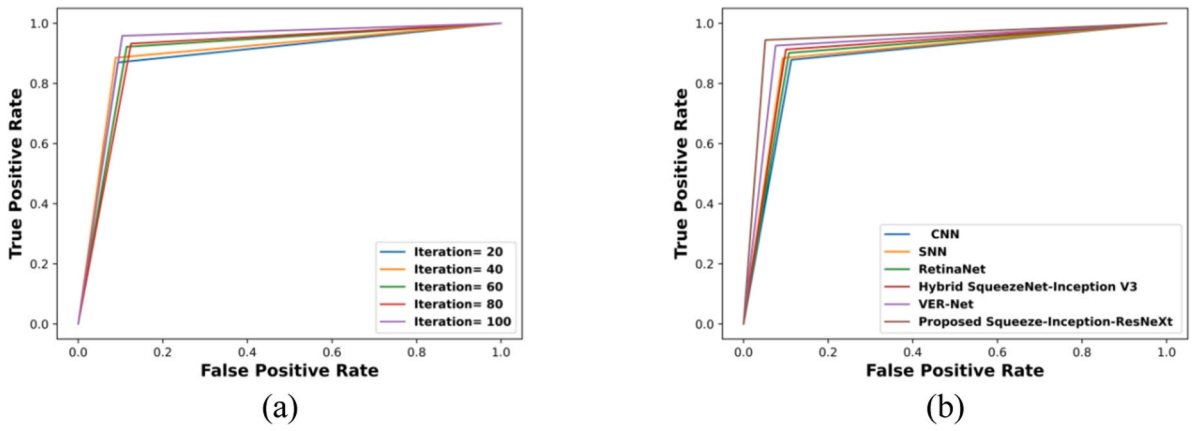


**Fig. 8.** RoC of model a) analysis of proposed Squeeze-Inception-ResNeXt b) Comparative analysis.

**Table 1**
Statistical analysis.

| Methods | CNN | SNN | RetinaNet | Hybrid SqueezeNet-Inception V3 | VER-Net | Squeeze-Inception-ResNeXt |
|---|---|---|---|---|---|---|
| **Best** | 0.918 | 0.928 | 0.9305 | 0.947 | 0.954 | 0.978 |
| **Mean** | 0.8858 | 0.893 | 0.896 | 0.910 | 0.915 | 0.940 |
| **Variance** | 0.03238 | 0.0345 | 0.0340 | 0.037 | 0.038 | 0.038 |

other approaches including CNN, SNN, RetinaNet, and Hybrid SqueezeNet-Inception V3 yielded results of 0.917, 0.927, 0.931, VER-Net was 0.954 and 0.947. Fig. 6(b) exhibited a comparative evaluation based on sensitivity. Squeeze-Inception-ResNeXt obtained a sensitivity of 0.933 for 70 % of training data, while SNN, Hybrid SqueezeNet-Inception V3, and CNN obtained 0.897, 0.919, and 0.892. In Fig. 6(c), a comparative analysis based on specificity was exhibited. While Squeeze-Inception-ResNeXt attained a specificity of 0.901 for 60 % of training data, CNN, SNN, RetinaNet, and Hybrid SqueezeNet-Inception V3 acquired specificities of 0.842, 0.845, 0.850, and 0.862. Squeeze-Inception-ResNeXt demonstrated a specificity of 0.937 for 80 % of training set, compared to 0.875 and 0.862 for RetinaNet and CNN.

Fig. 7 displays confusion matrix, which compares actual and predicted labels to assess performance of classification method. Matrix includes four categories: Normal, Adenocarcinoma, Large Cell Carcinoma, and Squamous Cell Carcinoma. It is based on 1402 testing samples to identify and categorize lung cancer. Matrix was generated using 80 % of training set, demonstrating that proposed method achieves an overall accuracy of 94.4 % for lung cancer detection.

Fig. 8 exemplifies ROC curves used for performance and comparative analysis of model. Fig. 8(a) presents ROC analysis for proposed Squeeze-Inception-ResNeXt model, which conquered a TPR of 0.91 and an FPR of 0.06 at iteration 60, and a TPR of 0.92 with an FPR of 0.13 at iteration 80. Fig. 8(b) presents ROC curves for various methods, including CNN, SNN, RetinaNet, and Hybrid SqueezeNet-Inception V3. The ROC curve for presented technique shows superior performance, with a higher TPR for a given FPR, highlighting its exceptional effectiveness in prediction tasks. Presented technique achieved an ROC of 0.97, while CNN, SNN, RetinaNet, and Hybrid SqueezeNet-Inception V3 achieved ROCs of 0.87, 0.91, 0.93, and 0.95.

Table 1 demonstrates the statistical analysis. Here, Squeeze-Inception-ResNeXt performs better than the other models based on the provided performance metrics. It has the highest best performance value at 0.978, which is considerably higher compared to other methods, like CNN (0.918), SNN (0.928), RetinaNet (0.931), Hybrid SqueezeNet-Inception V3 (0.947), and VER-Net (0.954). Additionally, it also has the highest mean value at 0.940, indicating consistent and reliable performance. The variance for Squeeze-Inception-ResNeXt is 0.038, which, although higher than some other models, is still within an acceptable range.

Table 2 presents an evaluation of various methodologies of training data. In this scenario, Squeeze-Inception-ResNeXt surpassed CNN by 6.14 % and Hybrid SqueezeNet-Inception V3 by 3.07 % in terms of accuracy. Squeeze-Inception-ResNeXt outperformed RetinaNet by 2.65 % and outperformed SNN by 3.56 % in terms of sensitivity. This approach executed 6.67 % superior performance than CNN and 4.31 % higher specificity when compared to Hybrid SqueezeNet-Inception V3.

## 5. Conclusion

- The study intends to present a classification method for lung diseases. It involves converting color spaces, augmenting data, scaling, and normalizing images during preprocessing.
- Features are extracted using a CNN based on SMA. Subsequently, Squeeze-Inception V3 is utilized to identify lung cancer.
- Additionally, ResNeXt is paired with Squeeze-Inception V3 to classify lung disorders into three categories: Squamous cell carcinoma, large cell carcinoma, and Adenocarcinoma.
- Also, SMA is employed in training the Squeeze-Inception-ResNeXt model, which is being developed for the categorization of lung cancer.
- The objective is to enhance the model's overall efficiency and performance in DL tasks.

**Table 2**
Comparative discussion.

| Methods | CNN | SNN | RetinaNet | Hybrid SqueezeNet-Inception V3 | VER-Net | Squeeze-Inception-ResNeXt |
|---|---|---|---|---|---|---|
| Accuracy | 0.917 | 0.928 | 0.931 | 0.947 | 0.954 | **0.977** |
| Sensitivity | 0.941 | 0.946 | 0.955 | 0.963 | 0.970 | **0.981** |
| Specificity | 0.909 | 0.914 | 0.925 | 0.932 | 0.940 | **0.974** |

- Experimental findings demonstrate that proposed method surpasses traditional techniques, achieving 97.7 % accuracy, 98.1 % sensitivity, and 97.4 % specificity.
- These outcomes underscore the effectiveness of Squeeze-Inception-ResNeXt model in classifying lung diseases.
- In future, the application of the Squeeze-Inception-ResNeXt model can be explored in other medical imaging tasks, such as brain tumor or cardiac disease classification. Also, the integration of the model with other diagnostic tools can be investigated and enhance its performance with larger, more diverse datasets.

## Ethical approval

Not Applicable.

## Informed consent

Not Applicable

## Funding

This research did not receive any specific funding.

## Author Contribution

All authors have made substantial contributions to conception and design, revising the manuscript, and the final approval of the version to be published. Also, all authors agreed to be accountable for all aspects of the work in ensuring that questions related to the accuracy or integrity of any part of the work are appropriately investigated and resolved.

## CRediT authorship contribution statement

**G Geethu Lakshmi:** Project administration. **Nagaraj P.:** Data curation.

## Declaration of Competing Interest

The authors declare no conflict of interest.

## Acknowledgements

I would like to express my very great appreciation to the co-authors of this manuscript for their valuable and constructive suggestions during the planning and development of this research work.

## References

Alakwaa, Wafaa, Nassef, Mohammad, Badr, Amr, 2017. Lung cancer detection and classification with 3D convolutional neural network (3D-CNN). Int. J. Adv. Comput. Sci. Appl. 8 (8).

Alnowami, Majdi, Taha, Eslam, Alsebaeai, Saeed, Muhammad Anwar, Syed, Alhawsawi, Abdulsalam, 2022. MR image normalization dilemma and the accuracy of brain tumor classification model. J. Radiat. Res. Appl. Sci. 15 (3), 33–39.

Bi, Zhicheng, Cao, Peng, 2021. Color space conversion algorithm and comparison study. J. Phys.: Conf. Ser. 1976 (1), 012008 (IOP Publishing).

BR, Sampangi Rama Reddy, Sen, Sumanta, Bhatt, Rahul, Dhanetwal, Murari Lal, Sharma, Meenakshi, Naaz, Rohaila, 2024. Stacked neural nets for increased accuracy on classification on lung cancer. Meas.: Sens. 32, 101052.

Chest CT-Scan images Dataset. ⟨https://www.kaggle.com/datasets/mohamedhanyyy/chest-ctscan-images⟩, (Accessed July 2022).

Crasta, Lavina Jean, Neema, Rupal, Pais, Alwyn Roshan, 2024. A novel deep learning architecture for lung cancer detection and diagnosis from computed tomography image analysis. Healthc. Anal. 5, 100316.

Dharavath, Krishna, Amarnath, G., Talukdar, Fazal A., Laskar, Rabul H., 2014. Impact of image preprocessing on face recognition: a comparative analysis. In: 2014 International Conference on Communication and Signal Processing. IEEE, pp. 631–635.

Dwivedi, Sandeep A., Borse, R.P., Yametkar, Anil M., 2014. Lung cancer detection and classification by using machine learning & multinomial Bayesian. IOSR J. Electron. Commun. Eng. (IOSR-JECE) 9 (1), 69–75.

Kalaivani, N., Manimaran, N., Sophia, S., Devi, D.D., 2020. Deep learning based lung cancer detection and classification. IOP Conf. Ser.: Mater. Sci. Eng. 994 (1), 012026 (IOP Publishing.

Kumar, Deepak, Kukreja, Vinay, 2021. N-CNN based transfer learning method for classification of powdery mildew wheat disease. In: 2021 International Conference on Emerging Smart Computing and Informatics (ESCI). IEEE, pp. 707–710.

Li, Liangyu, Yang, Jing, Por, Lip Yee, Khan, Mohammad Shahbaz, Hamdaoui, Rim, Hussain, Lal, Iqbal, Zahoor, et al., 2024. Enhancing lung cancer detection through hybrid features and machine learning hyperparameters optimization techniques. Heliyon 10.

Li, Qiang, Chen, Lei, Li, Xiangju, Lv, Xiaofeng, Xia, Shuyue, Kang, Yan, 2020a. PRF-RW: a progressive random forest-based random walk approach for interactive semi-automated pulmonary lobes segmentation. Int. J. Mach. Learn. Cybern. 11 (10), 2221–2235.

Li, Shimin, Chen, Huiling, Wang, Mingjing, Heidari, Ali Asghar, Mirjalili, Seyedali, 2020b. Slime mould algorithm: a new method for stochastic optimization. Future Gener. Comput. Syst. 111, 300–323.

Liu, Bei, Yu, Huiqing, Zeng, Xiaoping, Zhang, Dan, Gong, Juan, Tian, Ling, Qian, Junhui, Zhao, Leilei, Zhang, Shuya, Liu, Ran, 2021. Lung cancer detection via breath by electronic nose enhanced with a sparse group feature selection approach. Sens. Actuators B: Chem. 339, 129896.

Mahum, Rabbia, Al-Salman, Abdulmalik S., 2023. Lung-RetinaNet: lung cancer detection using a RetinaNet with multi-scale feature fusion and context module. IEEE Access 11, 53850–53861.

Maleki, Negar, Niaki, Seyed Taghi Akhavan, 2023. An intelligent algorithm for lung cancer diagnosis using extracted features from Computerized Tomography images. Healthc. Anal. 3, 100150.

Meena, Gaurav, Kumar Mohbey, Krishna, Kumar, Sunil, 2023. Sentiment analysis on images using convolutional neural networks based Inception-V3 transfer learning approach. Int. J. Inf. Manag. Data Insights 3 (1).

Nair, Sneha S., Devi, V.N.Meena, Bhasi, Saju, 2024. Enhanced lung cancer detection: Integrating improved random walker segmentation with artificial neural network and random forest classifier. Heliyon 10 (7).

Ozdemir, Onur, Russell, Rebecca L., Berlin, Andrew A., 2019. A 3D probabilistic deep learning system for detection and diagnosis of lung cancer using low-dose CT scans. IEEE Trans. Med. Imaging 39 (5), 1419–1429.

Ram, Sundaresh, Tang, Wenfei, Bell, Alexander J., Pal, Ravi, Spencer, Cara, Buschhaus, Alexander, Hatt, Charles R., et al., 2023. Lung cancer lesion detection in histopathology images using graph-based sparse PCA network. Neoplasia 42, 100911.

Saha, Anindita, Ganie, Shahid Mohammad, Dutta Pramanik, Pijush Kanti, Yadav, Rakesh Kumar, Mallik, Saurav, Zhao, Zhongming, 2024. VER-Net: a hybrid transfer learning model for lung cancer detection using CT scan images. BMC Med. Imaging 24 (1), 120.

Schiller, Herbert B., Montoro, Daniel T., Simon, Lukas M., Rawlins, Emma L., Meyer, Kerstin B., Strunz, Maximilian, Vieira Braga, Felipe A., et al., 2019. The human lung cell atlas: a high-resolution reference map of the human lung in health and disease. Am. J. Respir. Cell Mol. Biol. 61 (1), 31–41.

Singh, Gur Amrit Pal, Gupta, P.K., 2019. Performance analysis of various machine learning-based approaches for detection and classification of lung cancer in humans. Neural Comput. Appl. 31 (10), 6863–6877.

Xie, Saining, Girshick, Ross, Dollár, Piotr, Tu, Zhuowen, He, Kaiming, 2017. Aggregated residual transformations for deep neural networks. In: Proceedings of the IEEE Conference on Computer Vision and Pattern Recognition, pp. 1492–500.

Zhu, Xuefeng, Feng, Zao, Fan, Yugang, Ma, Jun, 2022. A multiple-blockage identification scheme for buried pipeline via acoustic signature model and SqueezeNet. Measurement 202, 111671.